Analysis of Restraints to Translational and Rotational Motion from the Geometry of Contact *

Raju S. Mattikalli Pradeep K. Khosla

Engineering Design Research Center
and The Robotics Institute
Carnegie Mellon University
Pittsburgh, PA 15213

In Proceedings ASME Winter Annual Meeting, Atlanta Dec. 1991. DE-Vol. 39, Issues in Design Manufacture/Integration. ASME 1991

Keywords: assembly planning, subassembly identification, instantaneous kinematics, direction of translation, direction sphere, axis of rotation, tangent plane enhanced constraint map

Abstract

The automatic generation of high-level assembly plans from geometric models makes extensive use of restraints imposed by components on one another. The geometry of contact can be used to find the nature of these restraints. In this paper, we present a method to determine restraints to translational and rotational motion of planar as well as 3-D objects. A set of parameters that represent any possible translational/rotational motion is identified. A geometric representation of the space of motion parameters ($\mathcal{M}_a$) is created. Restraints due to individual mating surface elements are computed by identifying subspaces in $\mathcal{M}_a$ which represent motion parameters that are 'disallowed' due to the contact. These are then superposed to generate the required solution. Restraints that are redundant are easily identified and are not computed. Information about restraints is used extensively in assembly planning - to determine degrees-of-freedom of components and subassemblies, to analyze the stability of subassemblies, to plan proper grasps, etc. We believe that the proposed representation can be used effectively in making these evaluations, taking us closer to generating correct assembly plans.

*This research was supported in part by the Engineering Design Research Center an NSF Engineering Research Center at Carnegie Mellon University

Notation

dof	degree of freedom
$\Re^2$	two dimensional Euclidean space
$\Re^3$	three dimensional Euclidean space
$\mathcal{M}_a$	space of *all* motion parameters
$\mathcal{M}_p$	space of *permissible* motion parameters
$\mathcal{M}_d$	space of *disallowed* motion parameters
$\mathcal{M}^+$	(for planar rotations) space of motion parameters parallel to +Z
ℓ	line in $\mathcal{M}$ that marks the boundary between $\mathcal{M}_d$ and $\mathcal{M}_p$
$\vec{r}$, $\vec{d}$	direction vector of the axis of rotation
$\vec{p}$	position vector of a point on the axis of rotation
$\mathcal{P}$	an arbitrary point on a plane tangent to $\vec{d}$
C^A	center of curvature at point A on a curve
(θ, ϕ, x, y)	algebraic representation of an axis of rotation
T_p	plane tangent to the direction sphere at point p
$\mathcal{S}_f$	constraint sphere generated by contact face f

1 Introduction

The increased use of computers in design and manufacture has lead to a gradual reduction in product lead time. Software tools that evaluate designs for various downstream activities, including manufacture, assembly, testing, packaging, etc. are making it easier for designers to anticipate modifications to the design resulting from downstream concerns, upfront during early design stages. Of interest to us is the process of assembly. Evaluation of a design for its assemblability requires knowledge of the assembly plan (as well as knowledge of the capabilities of the assembly facilities). Assembly plans can be automatically generated from geometric models of the design. These plans can also be used to rapidly program assembly facilities.

Lee and Ko[1] generated assembly plans based on qualitative descriptions of the kind of mating between components (namely against, fits, tight-fits and contact). De Fazio and Whitney[2] have described an interactive method for generating all assembly sequences, based on the *order* in which assembly operations are performed. De Mello and Sanderson[3] proposed the AND/OR graph as a means of generating and representing assembly plans. These approaches essentially use connectivity and precedence knowledge to produce assembly plans in terms of an *ordering* of components. Other efforts take a more geometric approach, generating assembly plans from *disassembly* simulations. Sedas and Talukdar[4] used a stick model to represent spatial occupation and generated disassembly motion plans. Hoffman[5] derived freedom of components and their motion along primary axes using ray casting techniques. In an earlier paper [6], the authors have described a software system that takes as input a geometric model of a mechanical system/assembly (MSA) and automatically generates high level assembly plans in terms of *assembly tasks*. To generate the assembly plan, the MSA is *disassembled* using a strategy based on kinematic constraints between mating parts. The disassembly method involves two main steps : (a) identifying subassemblies for disassembly based on their degrees-of-freedom (*dof*s) (and other criteria), and (b) using these *dof*s to generate a series of geometrically correct translational and rotational disassembly motions.

In [6, 5] and other efforts, translational *dof*s were assumed to exist only along the local coordinate directions; thus only the coordinate directions were tested for translational motion. Similarly, it was assumed that rotations would occur only about axes that coincide with the local coordinate axes. In this paper, we present an approach to determine translational *dof*s of a subassembly along arbitrary directions. Also, a method to determine rotational *dof*s along arbitrary axes in space is presented. These methods compute **restraints** to instantaneous motion from the geometry of contact between objects. Restraints due to individual mating surface elements are computed; these effects are then superposed to generate the required *dof*s. In both of the above methods, a geometric realization of the space of all possible motion parameters ($\mathcal{M}_a$) is constructed. $\mathcal{M}_p$ is a subspace in $\mathcal{M}_a$ that represents all permissible motion parameters ($\mathcal{M}_p \subseteq \mathcal{M}_a$). If an object has no mating surfaces, $\mathcal{M}_p = \mathcal{M}_a$. A mating surface element prevents the object from moving along a certain well defined set of directions which is expressed in terms of motion spaces as $\mathcal{M}_a$. The subspace over which motion is disallowed is referred to by $\mathcal{M}_d$. Thus each additional mating surface element reduces the space $\mathcal{M}_p$ and expands the space $\mathcal{M}_d$ such that the following relations are satisfied

$$\mathcal{M}_a = \mathcal{M}_p \cup \mathcal{M}_d \quad \& \quad \mathcal{M}_p \cap \mathcal{M}_d = \emptyset \tag{1}$$

After all effects have been considered, $\mathcal{M}_p$ is the solution space.

Reuleaux [7] identified the 'kinematic pair' and studied the geometric form of these pairs. He observed that there exists some general principle underlying the spatial arrangement of contact surfaces so as to maintain their mutual positions. He analyzed the effect of point contact on translational and rotational motion of *planar* objects. The field of restraint (which consists of the directions in which motion is prevented) for a point of contact was derived. Consider the planar object A with a point contact at *a* (as shown in figure 1(a)). Figure 1(b) shows the fields of restraints on translation; motion is prevented along

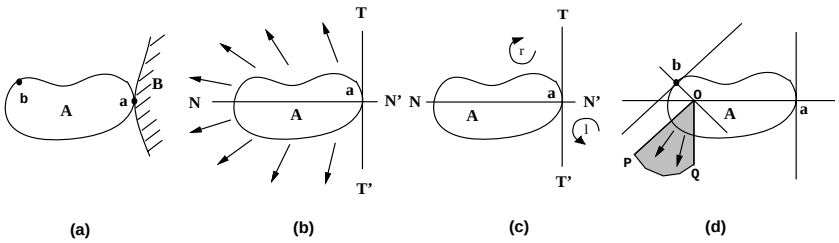

Figure 1: Reuleaux's analysis of restraints **(a)** A planar object *A* with contact at *a*, **(b)** The field of restraint to translations consists of directions between *TN'T'* **(c)** Restraints on counterclockwise (NTN') and clockwise turning (NT'N') **(d)** The field of sliding (shown shaded) due to multiple contacts.

directions between *TN'T'* due to contact at *a*. Calculation of restraints for two points of contact (*a* and *b*) is shown in figure 1(d). The analysis of restraints against turning proceeds along similar lines. A single point of restraint was shown to produce restraints on the fields of clockwise and anticlockwise turning as shown in figure 1(c). Clockwise turning is permitted in the region above (and including) line NN' whereas anticlockwise turning is permitted in the region below (and including) line NN'.

The work presented in this paper can be viewed as an extension of Reuleaux's work to objects in $\Re^3$. It makes three important contributions. First, the extension to $\Re^3$ which allows general translational and rotational motion. Second, a compact representation (which is geometric in nature) of the space of all possible translational and rotational axes is proposed. Third, the work presents an analysis of restraints not only from *point* contacts, but also from contact extending over *surfaces*. This work is motivated by our attempt to automatically generate assembly motion plans. As components move, mating conditions change. A representation of the restraint imposed by each surface in terms of its direction normal is created. The net restraint on the motion of a body is computed by transforming restraints due to each contact surface to a common coordinate frame and then superposing them.

2 Related Work

Cai [8] studied the kinematics of bodies in contact. Allowing for combined rolling and sliding at the point of contact, the author developed relationships for the motion of the moving body in connection with the surface curvature. Trajectories of two imaginary points (one on the moving and the other on the stationary objects) are defined. By specifying the trajectories of the imaginary contact points, along with the instantaneous orientation and sliding of the moving body, the trajectory of the moving object was determined.

Ohwovoriole [9] used the theory of screws to study the kinematics of the relative motion of contacting bodies. He introduced the notion of *total freedom* which describes all possible relative motions between two parts, in contrast to the restrictions of Cai's work that analyzed bodies which must maintain contact. To study relative motion the following method is adopted. The contact between a body and another is modeled as a set of wrenches; the motion of the body is represented by a twist; an expression for the virtual work done by the wrenches in the presence of the twist is obtained in terms of the unknown twist and known wrenches. By requiring that the virtual work be positive, inequalities are obtained, one for each wrench. These when solved give the unknown twist coordinates. Thus the displacement that the body is allowed to incur in the presence of the contacts can be obtained. In dealing with planar motion, the method used by Reuleaux [7] is simpler and provides identical results. The simplicity is gained by analyzing directly the effect of contact on permissible motion (as against first obtaining forces of restraint due to contact and then

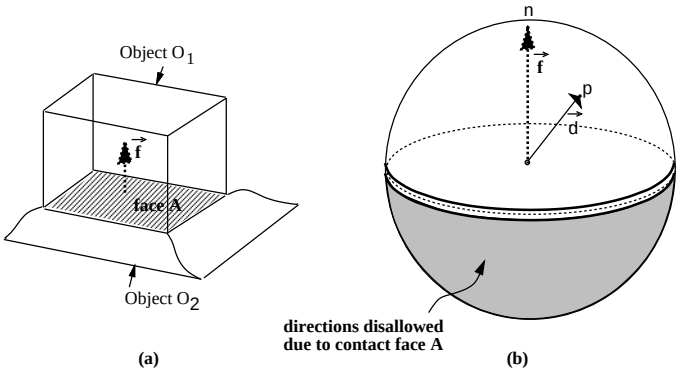

Figure 2: **(a)** An object with its mating face (face A) shown shaded, **(b)** The direction sphere, shown shaded are directions disallowed by mating face.

analyzing the motions permitted in the presence of these forces). Our work attempts to make use of the simplicity provided by Reuleaux's method and extend it to the motion of objects in $\Re^3$.

3 Translational Degrees of Freedom

Given the geometry of contact between an assembly (A) and another assembly (B), to find directions along which A possesses instantaneous translational motion relative to B. A representation of the space of all possible directions for translational motion is constructed. The effect of each mating element on these directions is calculated next.

Consider a sphere of unit radius (as shown in figure 2(b)). Construct a unit vector ($\vec{d}$) with its tail at the center of the sphere and its head at a point (p) on the surface of the sphere. We can refer to this vector by referring to the point p on the sphere. In a similar way, any arbitrary direction vector can be mapped onto a point on the unit sphere. This mapping of direction vectors to points on a sphere is bijective (one-to-one and onto) and can be used to represent all directions in $\Re^3$. The points on the surface of the sphere correspond to $\mathcal{M}_a$. This sphere will be referred to as the *direction sphere*.

The effect of a single mating face (figure 2(a)) on the space of allowed directions for translation is shown in figure 2(b). The hemisphere that is shaded ($\mathcal{M}_d$) is an open set of points. All directions that lie in this hemisphere are translation directions that are disallowed by contact over the face *A*. The complement of this set of directions ($\mathcal{M}_p$) is the set of allowed directions. For multiple contact faces, a superposition of the restraint hemispheres produced by each face of contact produces the set of disallowed directions (shown in figure 3). In this case, the object possesses translational *dof*s along directions represented by the arc *abc*.

4 Rotational Degrees of Freedom

Given the geometry of contact between an assembly (A) and another assembly (B), to find axes about which *A* possesses instantaneous rotational motion relative to *B*. An arbitrary rotational axis can be defined by a direction vector $\vec{d}$ and a position vector $\vec{p}$ (a point through which the axis of rotation passes). The proposed method is similar to that for translational motion. The method will be introduced by applying it to planar polygonal objects, followed by general planar objects and then to three dimensional polyhedral objects.

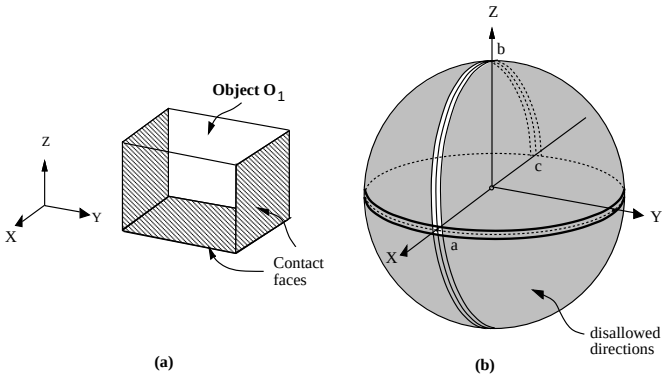

Figure 3: Superposition of constraints **(a)** An object with 3 mating faces (shown shaded), **(b)** Net effect of the 3 mating faces on translational *dof*s. Non-shaded portion shows *dof*s (arc *abc*.)

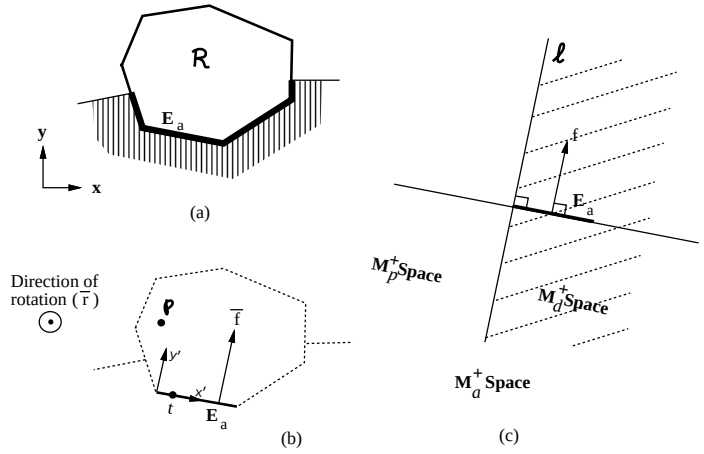

Figure 4: Rotational Restraints on planar objects **(a)** A polygon with its mating conditions, **(b)** A single mating element E_a, **(c)** Anticlockwise rotation is disallowed about axes that lie in the shaded region.

4.1 Rotational *dof*s for planar objects

4.1.1 Polygonal Objects

Consider a polygonal object $\mathcal{R}$ in the XY plane (figure 4(a)) which has mating constraints as shown. Consider an axis of rotation $(\vec{r}, \vec{p})$ where $\vec{r}$ is the direction vector and $\vec{p}$ the position vector of a point on the axis. For planar objects, $\vec{r}$ can be parallel to either the +Z or -Z coordinate directions. Although the range of $\vec{p}$ could be the space $\Re^3$, for a given $\vec{r}$ it would suffice if $\vec{p}$ is restricted to a plane that is perpendicular to $\vec{r}$. Thus we observe that two planes (one for each direction of $\vec{r}$) are a sufficient (geometric) representation of the space of all possible rotational axes for planar objects. The plane corresponding to the +Z coordinate direction is referred to as $\mathcal{M}_a^+$. $\mathcal{M}_a^-$ is the corresponding space for rotational axes in the -Z coordinate direction with $\mathcal{M}_a = \mathcal{M}_a^+ \cup \mathcal{M}_a^-$. Consider the mating element on $\mathcal{R}$ represented by edge E_a with inward normal $\vec{f}$ (as shown in figure 4(b)). The influence of E_a on allowed axes of rotation is obtained by identifying region $\mathcal{M}_d$ within $\mathcal{M}_a$.

To find $\mathcal{M}_d$ due to E_a refer to figure 4(b). Let t be an arbitrary point on E_a. A rotation about an arbitrary

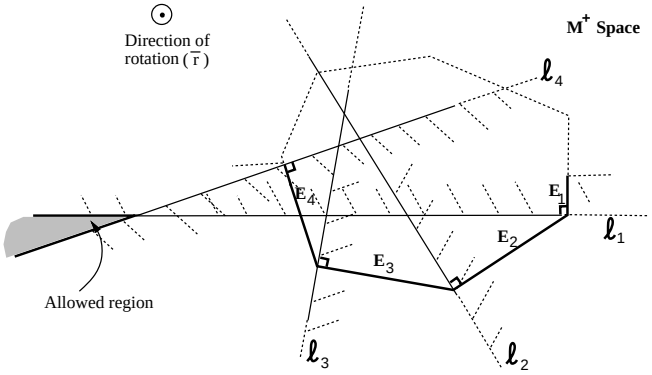

Figure 5: Superposition of individual constraints due to contact over edges.

point $\wp$ along direction $\vec{r}$ (the +Z direction in this case) is disallowed if

$$(\overline{r} \times \overline{\wp t}) \,.\, \overline{f} \;<\; 0 \qquad\qquad \forall t \in E_a \tag{2}$$

which is the scalar triple product of the vectors $\overline{r}, \overline{\wp t}$ and $\overline{f}$. It can be shown that any rotation in an anticlockwise direction is disallowed by the mating element E_a if they lie in the half plane to the right of line ℓ (shown shaded) in 4(c). Other mating edges impose similar restrictions on permissible axes of rotation. A superposition of all these subspaces produces the subspace of disallowed axes $\mathcal{M}_d^+$. The complement of this subspace with respect to $\mathcal{M}_a^+$ gives $\mathcal{M}_p^+$. To obtain the solution $\mathcal{M}_p^+$, a set of inequalities (one for each edge) of the form of (2) need to be solved. The solution to simultaneous linear inequalities can be considered to be one of *intersection of half planes*. An important property of the intersection of half planes is that the result is always a convex polygon. [10] describes a method which adopts a divide and conquer approach whose time complexity is $\mathcal{O}(N \ln N)$. Details can be found in [10].

Shown in figure 5 is the result of superposing the constraints due to individual mating edges. It shows a polygon whose edges $E_1, \ldots, E_4$ are mating edges. Lines $\ell_1, \ldots, \ell_4$ define the constraints on rotation imposed by each of the edges. For each ℓ the half plane shown hatched is the disallowed region. The advantage of using a geometric realization over an algebraic one is to be able to predict as to which constraints are redundant. The regions constrained by edges E_2 and E_3 are contained within those imposed by E_1 and E_4 rendering them *redundant*. In what follows, we shall make use of the fact that some constraints are redundant and need not be accounted for to begin with. We identify those constraints that define the boundary of the permissible subspace $\mathcal{M}_p^+$; the remaining constraints are ignored.

4.1.2 General Planar Objects

Shown in figure 6(a) is an object in $\Re^2$ bounded by curves. Consider rotations perpendicular to the plane of the paper in an anticlockwise direction. For convenience, we shall drop the superscript from the notation for the space of motion parameters ($\mathcal{M}$), though in the following paragraphs only anticlockwise rotations are analyzed. Each point on the curve that mates with another object, produces a constraint on the space $\mathcal{M}_p$. Not all points of contact need to be examined since some produce redundant constraints. We shall identify segments of the boundary that produce redundant constraints and determine those points that directly define the bounds of $\mathcal{M}_d$ without having to solve for inequalities such as (2). The curve of contact is divided into segments where the curvature is either decreasing or increasing. Also divisions are made at points of inflexion. It is assumed that each curved segment possesses derivatives of at least the second order.

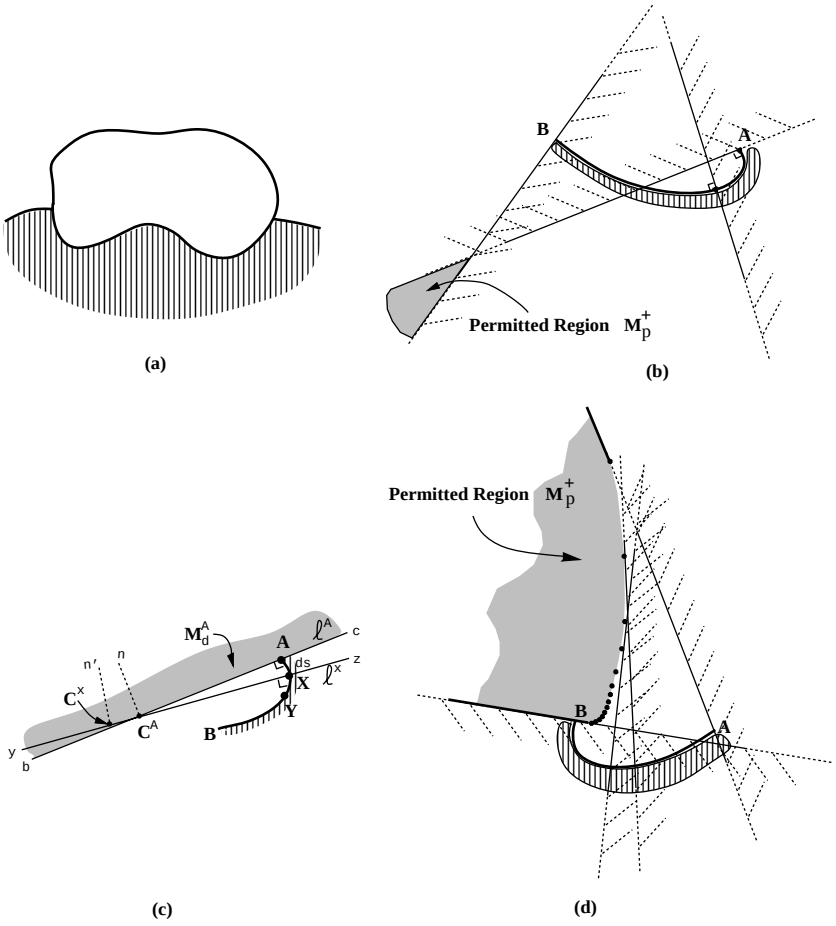

Figure 6: **(a)** A 2-D object with curved boundaries along with its mate (shown shaded), Calculating the permitted region due to a contact curve with **(b),(c)** decreasing curvature along AB, **(d)** increasing curvature along AB.

From the analysis of anticlockwise rotation with linear contact, it was shown that the line ℓ due to each edge is perpendicular to the edge. Figure 6(a) shows an object with mating contacts described by curves. The analysis for segments with increasing and decreasing curvatures are performed separately. Consider the segment of contact in figure 6(b) that has a non-increasing curvature from point A to point B. Let the center of curvature at point A be C^A (and the radius of curvature $\rho(A)$). Let the region excluded by A be $\mathcal{M}_d^A$ and the bounding line ℓ^A. Note that ℓ^A is normal to the curve at point A and passes through C^A. Consider a point X at a distance *ds* away from A (*s* is the curvilinear coordinate) as shown in figure 6(c). The normal to the curve at X passes through C^A (A and X are infinitesimally close). Since the curvature is decreasing (i.e. $d\rho/ds$ is positive), $\rho(X)$ is greater than $\rho(A)$. Thus C^X is located as shown in figure 6(c). The following two properties hold for any two adjacent points on the curve (in this case, points A and X in figure 6(c)).
Property 1: The portion of $\mathcal{M}_d^X$ in the quarter-plane defined by $y\,C^X\,n'$ (including the semi-infinite line $C^X\,n'$) lies entirely within $\mathcal{M}_d^A$.
Property 2: The portion of $\mathcal{M}_d^A$ in the quarter-plane defined by $c\,C^A\,n$ lies within $\mathcal{M}_d^X$.
In superposing the effect of points A and X, using property 1 it can be seen that the region enclosed between $z\,C^A\,c$ is the contribution made by the constraint at point X to M_d^A. Applying property 2 to point X and the next point along the curve(point Y), we can show that the contribution made by the constraint at point X is entirely enclosed within that made by point Y. Thus by induction over the entire range of points along the curve from point A to B, we can show that *the constraints imposed by the end-points of a segment with a non-increasing curvature make redundant the constraints imposed by points inbetween them.* Lines ℓ^A and ℓ^B thus are sufficient to define $\mathcal{M}_d$ due to segment AB.

Consider next a segment with an increasing curvature (figure 6(d)). Using points A and X as above, we can show that the portion of $\mathcal{M}_d^X$ beyond C^X is included within $\mathcal{M}_d^A$ and the portion of $\mathcal{M}_d^A$ below C^A is within $\mathcal{M}_d^X$. However note that point C^A itself is not included within $\mathcal{M}_d^X$. This holds for all adjacent points along AB. Hence for segments of contact with increasing curvature, the constraints imposed by the end points along with the locus of centers of curvature of points between them are sufficient to define $\mathcal{M}_d$.

To summarize, we have shown that by computing

1. constraints due to a certain set of contact points, and

2. the locus of centers of curvature over segments with decreasing curvature

we can determine $\mathcal{M}_d$ due to curvilinear contact between planar objects.

In section (4.2) we extend this method to polyhedral objects. Some interesting properties of the representation emerge, which are explored. Superposition of the $\mathcal{M}_d$s due to each of the contact elements is a challenging problem. Solutions to this problem are explored.

4.2 Rotational *dof*s for polyhedral objects

The method of analyzing rotational *dof*s for objects in $\Re^3$ is similar to that of analyzing planar objects. However, the geometric representation of the space $\mathcal{M}_a$ is more involved than that for planar objects. To represent an arbitrary axis in $\Re^3$, 4 independent scalars are required. To intuitively see as to why only 4 are required, consider this: two scalars are sufficient to specify a direction $\vec{r}$ (the azimuth angle θ, the zenith angle ϕ of spherical coordinates); two others specify a point q on the plane perpendicular to the direction. These 4 scalars define an axis parallel to $\vec{r}$ passing through point q. Any set of four or more scalars can be used to define an axis in space. In section (4.2.1), we present a representation that is geometrically realized. This realization is the key to the discovery of some important properties which lead to a compact computer representation of all possible axes of rotation. Subsequent analysis of rotational *dof*s is simplified as a result of compactness in the representation.

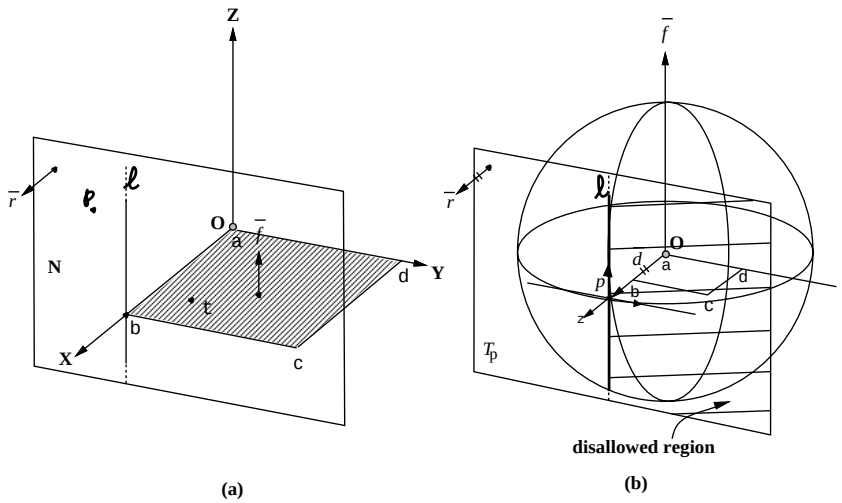

Figure 7: **(a)**Analysis of restraints on rotation along $\vec{r}$ due to mating face *abcd*, **(b)** The space $\mathcal{M}_a$ showing the disallowed region $\mathcal{M}_d$ in the direction $\vec{d}$.

4.2.1 Tangent Plane Enhanced Sphere

Consider the direction sphere as shown in figure (2). Unit vector ($\vec{d}$) has its tail at the center of the sphere and its head on point p on the surface. Imagine placing a plane (T_p) tangential to the sphere at point p. Define a local frame of reference on T_p at the point of contact with the sphere, with its Z axis along the direction vector $\vec{d}$ and its Y axis tangent to the longitude pointing north. An axis of rotation parallel to $\vec{d}$ can be represented by a point on T_p, expressed in terms of the local coordinate frame. If we construct planes tangential to all points on the sphere, we have a geometric representation for all possible axes of rotation. This is the space $\mathcal{M}_a$ for objects in $\Re^3$. The set (θ, ϕ, x, y) is an algebraic representation of the same.

4.2.2 Constraints on Permissible Axes of Rotation due to a Planar Contact Face

Consider the object with a single planar contact surface as shown in figure 2(a). The mating face is isolated and shown in figure 7(a). $\vec{r}$ is parallel to the X axis; N is a plane normal to $\vec{r}$. We will analyze the restraints on axes of rotation whose direction vector $\vec{d}$ is parallel to $\vec{r}$. Once this is obtained, we will analyze restraints on axes in other directions perpendicular to $\vec{f}$; finally the remaining directions will be considered. The tangent plane enhanced direction sphere ($\mathcal{S}_f$) is shown in figure 7(b). As shown, the sphere $\mathcal{S}_f$ is oriented such that its north-south axis is parallel to $\vec{f}$; this orientation is significant (as will become evident later). The center of the sphere is located at the origin O. The direction $\vec{r}$ corresponds to point p on the direction sphere (with $\vec{d}$ parallel to $\vec{r}$ as shown). The tangent plane T_p at point p on the sphere is shown. Consider a point $\wp$ on the plane N and an arbitrary point t on the rectangle *abcd*. We want to find a condition which disallows rotation about an axis in the direction of $\vec{r}$ passing through point $\wp$. As was the case for planar objects, the condition is as follows

$$(\overline{r} \times \overline{\wp t}) \,.\, \overline{f} \;<\; 0 \qquad\qquad \forall t \in \Box abcd \tag{3}$$

How does this condition manifest itself geometrically on plane T_p? It defines a region on plane T_p that represents $\mathcal{M}_d$ (shown shaded in figure 7(b)). Note that there is a close correspondence between planes N and T_p; a point on N transforms to exactly the same point on T_p. They are considered different because they exist in different spaces; N is a plane in $\Re^3$ whereas T_p is a part of the representation of rotational

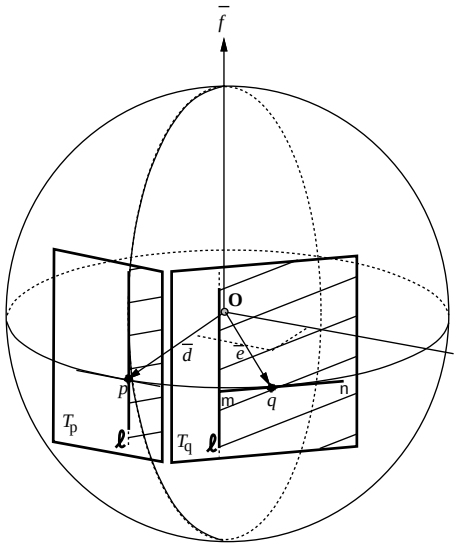

Figure 8: The constraint sphere showing subspaces (shaded) along directions $\vec{d}$ and $\vec{e}$ that are disallowed due to a single contact face.

axes. To determine $\mathcal{M}_d$, project *abcd* onto plane *N*. The projection is a line segment with end-points *b* and *c*. Construct line ℓ perpendicular to the projection and passing through *b*. To understand the physical interpretation of the results, consider the following. When rotated about an axis in the direction of $\vec{r}$, each point on *abcd* would trace out a circle centered on the axis in a plane perpendicular to the axis. Tangents drawn on these circles in the anticlockwise direction (when looking at the center of the sphere from point *p*) at points of contact with *abcd* represent the direction of instantaneous motion that is imparted to these points. Circles centered on axes that are in the left half plane of line ℓ impart instantaneous motions to *all* points on *abcd* that push the points away from contact. On the other hand, all circles centered in the right half plane would tend to push some points on *abcd* into the contact (which is physically impossible), making their centers "disallowed" points. Note that since points on the line ℓ are allowed, the space of disallowed points ($\mathcal{M}_d$) is an open set. Thus, inequality (3) is satisfied for all points to the right of line ℓ. This is shown shaded as the disallowed region in figure 7(b).

Thus far, we have obtained a subspace in $\mathcal{M}_a$ over which rotations are disallowed by face *abcd* along axes that are in the direction of $\vec{d}$. Next, we obtain the restraints by face *abcd* on other directions that are perpendicular to the face normal $\vec{f}$ (these directions lie on the equatorial plane of the sphere shown in figure 7(b)).

Consider an arbitrary direction $\vec{e}$ on the equator as shown in figure 8. The projection of *abcd* on the tangent plane T_q is segment *mn*. A line passing through *m* perpendicular to *mn* is constructed on plane T_q. Using arguments similar to the one presented for T_p, we can see that this line is ℓ, and the right half plane on T_q (shown shaded) represents $\mathcal{M}_d$. The above is true for any direction on the equatorial plane. It is apparent that line ℓ on the two planes T_p and T_q does not have the same location with respect to the local frames on the two planes. How does line ℓ vary along the equator? Consider the top view of rectangle *abcd* as shown in figure 9(a). $\vec{e}_1$ and $\vec{e}_2$ are two directions on the equator with an angular separation of α. By isolating quadrilaterals Obm_1p_1 and Obm_2p_2 (as shown in figure 9(b)) and superposing them (figure 9(c)), the relationship between the locations of ℓ on equatorial tangent planes is evident. It is given by the projection of a rotating vector $\overline{Ob}$, rotating in a direction opposite to that of the direction vectors.

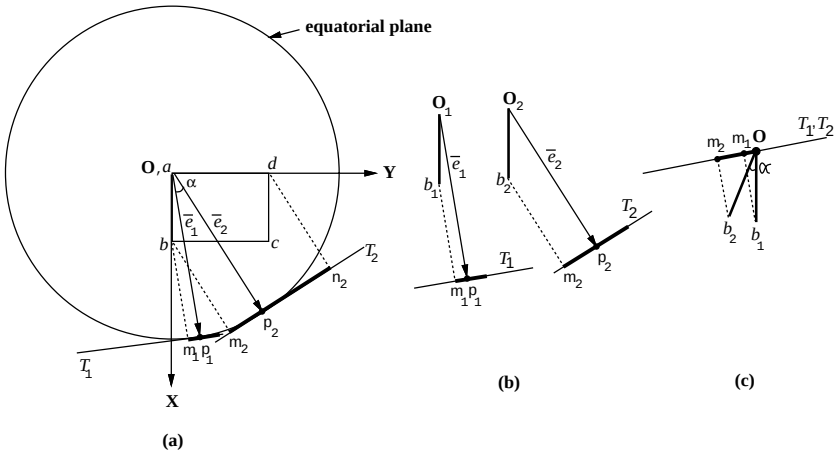

Figure 9: Calculating the variation of $\mathcal{M}_d$ along the equator. **(a)** Project *abcd* on two tangent planes, **(b)** Want to study the variation of *m* with respect to *p*, **(c)** Project rotating vector $\overline{Ob}$ to give variation of $\mathcal{M}_d$.

As we move along the equator in an anticlockwise direction and follow the projection of *abcd*, we can see that the location of ℓ on the tangent planes is not 'governed' by vector $\overline{Ob}$ alone. To illustrate this refer to figure 10 which shows a polygon *abcde*. Any point along arc AB is 'governed' by vector $\overline{Oa}$, arc BC by $\overline{Ob}$ and so on. To construct these arc segments, imagine moving the unit tangent vectors of each edge such that its tail is placed at the center of the sphere. These direction vectors define the zone of influence of each vertex of the face.

Let us now consider the influence of face *abcd* on directions other than those on the equator. Consider a direction ($\vec{r}$) in the northern hemisphere as shown in figure 11(a). As before, if $\wp$ is a point on the tangent plane *N* and *t* is an arbitrary point on *abcd*, then the condition that prevents rotations along direction $\vec{r}$ through point $\wp$ is

$$(\vec{r} \times \overline{\wp j}) \,.\, \vec{f} < 0 \qquad\qquad \forall_j \in \square abcd \tag{4}$$

In figure 11(b), the point *p* on the constraint sphere corresponds to direction $\vec{r}$. T_p is the associated tangent plane. To find the location of ℓ on T_p, perform the following construction (shown in figure 11(b)). Construct a plane (H_p) perpendicular to the equator passing through *p* and the origin of the sphere *O*. The intersection of this plane with the sphere passes through a longitude of the sphere on which *p* is located. $\overline{T}_p$ is the tangent plane at the point of intersection of this longitude with the equator. The point on *abcd* that governs ℓ on $\overline{T}_p$ is *b*. Note that H_p is perpendicular to both T_p and $\overline{T}_p$. We shall show that the line ℓ on T_p and ℓ on $\overline{T}_p$ have identical locations on their respective planes with respect to their local frames. Construct a plane H_b parallel to H_p passing through the governing point *b*. Since T_p is perpendicular to H_p which is parallel to H_b, plane T_p is perpendicular to plane H_b. Similarly $\overline{T}_p$ is perpendicular to H_b. The intersection of H_b with $\overline{T}_p$ defines a line. This line is perpendicular to the equator and passes through the projection of the governing point b on $\overline{T}_p$. This intersection thus coincides with line ℓ on $\overline{T}_p$. Let H_b intersect T_p at line ℓ'. It can be shown that the line ℓ' on T_p is the boundary of $\mathcal{M}_d$. Thus the intersection of plane H_b with T_p gives us the location of ℓ on T_p. Now each point on T_p is described with respect to the local reference frame, which is located on H_p and has its X axis perpendicular to H_p. Since the same plane (namely H_b) defines ℓ on T_p and $\overline{T}_p$ and because of the location of the reference frames on each of the tangent planes, we conclude that the equation of line ℓ on T_p and $\overline{T}_p$ with respect to their local frames is identical. The conclusion made above is a very significant one. Note that the direction $\vec{r}$ chosen was an arbitrary one. This

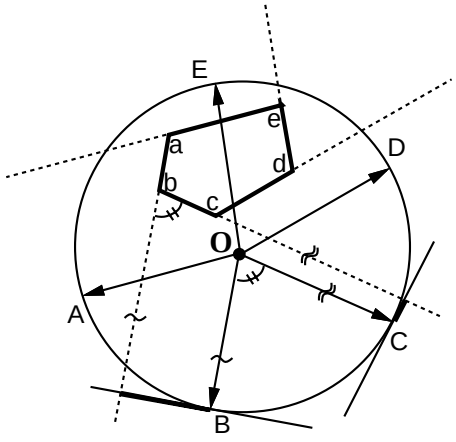

Figure 10: To determine arc segments on the equator that are governed by a single vertex, translate vectors along edges of the polygon to the center *O* of the sphere.

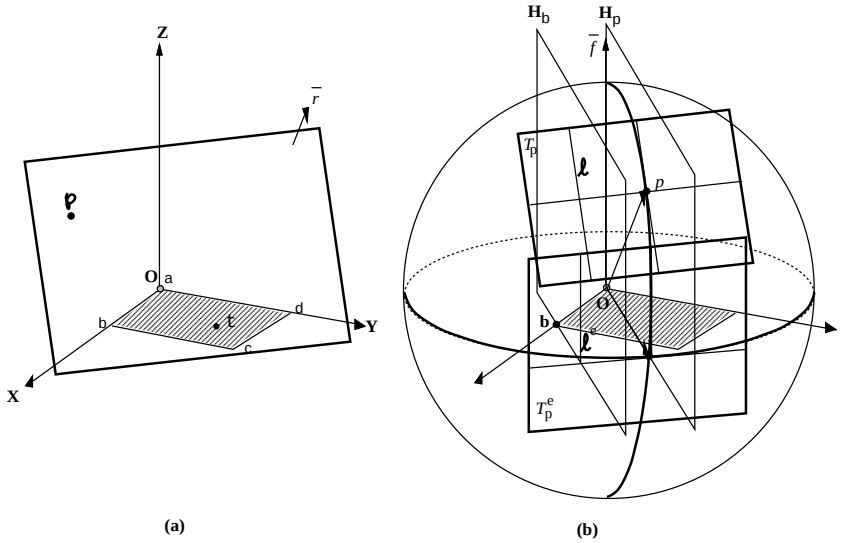

Figure 11: To study the constraints imposed by mating face *abcd* on rotational axes in the direction $\vec{r}$, **(a)** Mating face *abcd* with a plane *N* perpendicular to direction $\vec{r}$, **(b)** Construction to show that the constraint on T_p is identical to that on $\overline{T}_p$. These two planes are tangents on the same longitude.

proves an important property of allowable rotation axes,
Property 3 : *All directions along a longitude on the sphere have identical tangent planes due to a single contact face*.
The invariance of ℓ along a longitude makes it sufficient for us to represent only those tangent planes that lie on the equator.

Another important property of the line ℓ is its invariance to translations of face *abcd* in the direction of its normal. Consider figure 11(b). When *abcd* is translated in the direction of $\vec{f}$ it stays bounded between the planes H_p and H_b. Consider an axis represented by a point in the half plane to the left of ℓ on T_p (this point is in the allowed region). The effect of translating *abcd* by an arbitrary amount is to change the angle at which points on *abcd* are imparted instantaneous motion due to rotations about the axis. However no point is imparted motion against the direction of the vector $\vec{f}$. Similarly it can be seen that the influence of axes in the right half plane on the character of the instantaneous motion imparted to points on *abcd* remains unchanged. Hence
Property 4 : *Restraints to rotation remain unchanged when the contact face is translated in a direction parallel to its normal*.

What about translations within the plane of the face? It can be seen that the location of ℓ changes with translations in the plane. Even the vertex on *abcd* that governs the location of ℓ could change. For each translated position, the ℓs need to be recomputed using the method described earlier.

To recapitulate some of the salient features,

1. We have developed a representation for the space of all rotational axes,
2. We have developed a method for constraining the space of rotational axes due to the presence of a single surface element,
3. We discovered a useful property: the invariance of ℓ over axes that have the same azimuth angle,
4. Another useful property, namely the invariance of ℓ with translations of the face of contact along a direction normal to the face, was also proved,
5. translations of the contact face within the its plane requires the recomputation of ℓ.

The items (3) and (4) above are useful in superposing the constraints due to each contact face to get the rotational degrees-of-freedom of the part. In what follows we shall present a solution to the problem of computing the net *dof* of a part by superposing individual constraint spheres.

4.3 Superposition of Constraint Spheres

In section 4.2.2, to compute the restraints to rotation due to a single planar contact face, the constraint sphere $\mathcal{S}_f$ was aligned with its *Z* axis parallel to the face normal and was located with its origin in the plane of the face. Property 4 (in section 4.2.2) allows us to place the origin of $\mathcal{S}_f$ outside the plane of the face. However, the condition that the Z axis of a sphere be aligned with the inward normal of the contact face cannot be relaxed. Thus for objects with multiple contact faces, we have constraint spheres (one for each face) that are aligned along their respective face normals. The calculation of the net restraint at a point on the sphere involves (a) transforming the equation of the restraint boundaries of each of the spheres to the global coordinate frame, and (b) computing their intersection in the global frame. Let $\mathcal{S}_f$ be a constraint sphere oriented arbitrarily with respect to the global sphere $\mathcal{S}_g$.

Refer to figure 12. Frame *XYZ* is the global reference frame. The *Z* axis corresponding to point $\mathcal{Z}$ on the sphere $\mathcal{S}_g$. Let $X'Y'Z'$ be a reference frame attached to sphere $\mathcal{S}_f$. The Z' axis corresponds to point $\mathcal{T}$ on

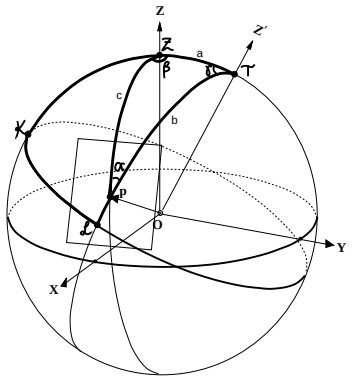

Figure 12: Construction to transform the restraints captured in a local sphere $\mathcal{S}_f$ to the global sphere $\mathcal{Z}_g$.

sphere $\mathcal{S}_g$. Given a point p in XYZ we want to calculate the restraints on rotation in the direction of p due to sphere $\mathcal{S}_f$. We know from section (4.2.2) that the restraints on rotation at a point on a sphere due to a single planar contact face is defined by line ℓ. A method to calculate ℓ at a point with respect to the local frame ($X'Y'Z'$ in this case) was described. We would like to obtain the location of ℓ at *p with respect to the global frame XYZ*. The X' axis (i.e. the 0 deg longitude for $\mathcal{S}_f$) is oriented such that it passes through the geodesic between points $\mathcal{T}$ and $\mathcal{Z}$. (In 3-D Euclidean space, a geodesic is the shortest line between two points on a mathematically derived surface). Arcs are drawn on the surface of $\mathcal{S}_g$ as shown in figure 12; point $\mathcal{K}$ is the intersection of the 0 deg longitude of $\mathcal{S}_f$ with its equator; $\mathcal{L}$ is the intersection of the longitude that passes through p with the equator. First the equation of ℓ at $\mathcal{L}$ is calculated with respect to $X'Y'Z'$. Thus ℓ at p is known using property 3 (again with respect to $X'Y'Z'$). This is transformed to the XYZ coordinates by a rotation of angle $(-\alpha)$.

To calculate ℓ at $\mathcal{L}$ with respect to $X'Y'Z'$, the length of arc $\mathcal{KL}$ is computed. This defines the longitude on $\mathcal{S}_f$ which passes through p. Using the method described in section (4.2.2), ℓ at $\mathcal{L}$ is calculated. To determine angle α, consider the spherical triangle $\mathcal{TZP}$. The spherical coordinates of points $\mathcal{T}$ ($\theta_\mathcal{T}$, $\phi_\mathcal{T}$), $\mathcal{Z}$ ($\theta_\mathcal{Z} = \pi/2$) and $\mathcal{P}$ ($\theta_\mathcal{P}$, $\phi_\mathcal{P}$) are known, with

$$\beta = |\theta_\mathcal{P} - \theta_\mathcal{T}| \tag{5}$$

$$\ell(\mathcal{TZ}) = a = (\pi/2) - \phi_T \tag{6}$$

$$\ell(\mathcal{ZP}) = c = (\pi/2) - \phi_P \tag{7}$$

Using spherical oblique triangle equations, we have

$$\alpha = X + Y \tag{8}$$

$$\gamma = X - Y \tag{9}$$

where

$$X = \tan^{-1} \frac{\cos(\beta/2)\ \cos[(a-c)/2]}{\sin(\beta/2)\cos[(a+c)/2]} \tag{10}$$

$$Y = \tan^{-1} \frac{\cos(\beta/2)\ \sin[(a-c)/2]}{\sin(\beta/2)\sin[(a+c)/2]} \tag{11}$$

The spherical triangle $\mathcal{TKL}$ is a right triangle (where the right angle is at $\mathcal{K}$). Therefore,

$$\ell(\mathcal{TK}) = \pi/2 \tag{12}$$

$$\ell(\mathcal{KL}) = \tan^{-1}(\sin b \ \tan\alpha) \tag{13}$$

Equations (8), (10), (11) and (13) give us the required values of $\ell(\mathcal{KL})$ and angle α.

Summarizing the results in terms of a computer implementation, we have shown is that for each face of contact, by storing

1. the geometry of the face,
2. the spherical coordinates of the normal of the face when represented on the global constraint sphere,
3. the partitioning of the equator of the constraint sphere of the face based on the regions 'governed' by a single vertex,

the space of disallowed axes of rotation $\mathcal{M}_d$ (which is given by ℓ) due to that face can be computed. By transforming the half planes defined by the ℓs due to each of the contact faces to a global frame and then computing their intersection, the convex region that represents $\mathcal{M}_p^{net}$ can be obtained.

Summary

Geometric models of designs play an important role not only in the specification of their shape, but also in the planning of their manufacture. This work addresses the process of assembly of designs. In the simulation and analysis of the assembly process, there is a need to represent restraints between components.

In this paper, we have presented a scheme for calculating and representing restraints on components due to contact with other components. Translational and rotational restraints are represented separately. A geometric representation of the space of all possible motion parameters is constructed within which a subspace of allowed motion parameters is computed.

The knowledge represented in this abstraction of the design plays a fundamental role in the simulation of assembly. To produce an assembly plan, we simulate a disassembly of the design. Selection of subassemblies uses knowledge of restraints in finding subassemblies that possess degrees-of-freedom. *Stability* considerations are also used in selecting subassemblies. Stability can be inferred from knowledge about restraints due to contact. Restraints are also used to plan grasps of *assemblies*. We believe that the representation of restraints that is proposed in this paper is an important step towards automated assembly planning and analysis.

References

[1] K. Lee and H. Ko, "Automatic assembly procedure generation from mating conditions," *CAD*, vol. 19, no. 1, pp. 3–10, 1987.

[2] D. Whitney and T. DeFazio, "Simplified generation of all mechanical sequences," *IEEE Journal of Robotics and Automation*, vol. RA-3, no. 6, December, 1987.

[3] L. H. de Mello and A. Sanderson, "And/or graph representation of assembly plans," *Technical Report, The Robotics Institute*, vol. CMU-RI-TR-86-8, 1986.

[4] S. Sedas and S. Talukdar, "Disassembly expert," *Technical Report, Engineering Design Research Center, Carnegie Mellon University*, vol. EDRC-01-03-87, 1987.

[5] R. Hoffman, "Automated assembly in a csg domain," *Proc. IEEE Conference on Robotics and Automation*, pp. 210–215, 1989.

[6] R. Mattikalli, P. Khosla, and Y. Xu, "Subassembly identification and motion generation for assembly: A geometrical approach," in *Proceedings of IEEE Conference on System Engineering*, pp. 399–403, 1990.

[7] F. Reuleaux, *The Kinematics of Machinery*. Macmillan 1876, Republished by Dover, 1963.

[8] C. Cai, "Instantaneous robot motion with contact between surfaces," Thesis STAN-CS-88-1191, Stanford Univ., January 1988.

[9] M. S. Ohwovoriole, *An extension of screw theory and its application to the automation of industrial assemblies*. PhD thesis, Stanford University, PhD Thesis, April 1980.

[10] F. P. Preparata and M. I. Shamos, *Computational geometry : an introduction*. New York: Springer-Verlag, 1985.